Astronomy & Astrophysics manuscript no. PML_Ziad_22468
September 19, 2013

Letter to the Editor

First results of the *PML* monitor of atmospheric turbulence profile with high vertical resolution

A. Ziad, F. Blary, J. Borgnino, Y. Fanteï-Caujolle, E. Aristidi, F. Martin, H. Lantéri, R. Douet, E. Bondoux, and D. Mékarnia

Laboratoire J.L. Lagrange UMR 7293, Université de Nice Sophia-Antipolis/CNRS/OCA, Parc Valrose 06108, Nice, France
e-mail: ziad@unice.fr

Received ; accepted

ABSTRACT

Aims. Future Extremely Large Telescopes will be certainly equipped with Wide-Field Adaptive Optics systems. The optimization of the performances of these techniques requires a precise specification of the different components of these AO systems. Most of these technical specifications are related to the atmospheric turbulence parameters, particularly the profile of the refractive index structure constant $C_N^2(h)$. A new monitor PML (Profiler of Moon Limb) for the extraction of the $C_N^2(h)$ profile with high vertical resolution and its first results are presented.
Methods. The PML instrument uses an optical method based on the observation of the Moon limb through two subapertures. The use of the lunar limb leads to a continuum of double stars allowing a scan of the whole atmosphere with high resolution in altitude.
Results. The first prototype of the PML has been installed at Dome C in Antarctica and the first results of the PML are presented and compared to radio-sounding balloon profiles. In addition of the $C_N^2(h)$ profile obtained with high vertical resolution, PML is also able to provide the other atmospheric turbulence parameters as the outer scale **profile**, the total seeing, the isoplanatic and isopistonic angles.

Key words. Atmospheric Turbulence – Atmospheric effects – Site testing – Adaptive Optics

1. Introduction

For the next generation of ground-based telescopes, the classical Adaptive Optics (AO) reaches its limitations mainly **when correction is needed over** a large field-of-view. Other AO concepts called Wide-Field Adaptive Optics (WFAO) have been proposed for this large field compensation in the perspective of future ELTs (Ellerbroek 2011, Hubin 2011). The optimization of the performances of the WFAO techniques requires a precise specification of the different components of these systems. Some of these technical specifications are related to the optical parameters of the atmospheric turbulence, particularly the $C_N^2(h)$ profile.

Moreover, recent studies (Costille & Fusco 2011) show that it is necessary to have access to $C_N^2(h)$ **profiles** with high vertical resolution for a better evaluation of the performance of a WFAO system.

Different instruments as radio-sounding balloons, SCIDAR, MASS, SLODAR and MOSP have been developed for $C_N^2(h)$ profile estimation. The balloons (Azouit et al. 2005) lead to estimated profiles with high vertical resolution but the measurements are sequential over the ascent time $\sim 2h$ and they remain expensive knowing they are lost after the flight. The SCIDAR (Fuchs et al. 1998) requires a large telescope ($\sim 2m$) and the resolution is low in the ground layer (GL). The other instruments lead to a low altitude resolution and/or are restricted to a part of the atmosphere (GL or free atmosphere (FA)).

A new instrument PML (Profiler of Moon Limb) initially known as PBL ("Profileur Bord Lunaire") has been developed for the extraction of the $C_N^2(h)$ profile with high vertical resolution from Moon limb fluctuations. The PML instrument is based on a differential method by observation of the lunar limb through two sub-apertures. The advantage of using the lunar limb is the presence of a continuum of double stars allowing the scan of the whole atmosphere with high resolution.

In this paper, the PML instrument is presented and its components described. The theoretical background of the extraction of $C_N^2(h)$ profile from PML measurements is presented. PML has been installed at Dome C in Antarctica in January 2011. The first results of PML obtained during this campaign are presented and compared to radio-sounding **balloon** profiles.

2. PML instrument

The PML is a new instrument for the extraction of the C_N^2 profile with high vertical resolution by use of an optical method based on the observation of the Moon limb. **This has** the advantage of offering a large number of angular separations required between two points of the edge allowing the scan the atmosphere with a very fine resolution. The PML instrument uses the differential method of a DIMM (Differential Image Motion Monitor) (Sarazin & Roddier 1990) based this time on the observation of the lunar limb instead of a bright single star, through two sub-apertures (Fig. 1). The angular correlation along the lunar limb of the differential distance between the two lunar edges leads to the $C_N^2(h)$ profile. The other parameters of turbulence are also accessible from this instrument as the profile of outer scale (Maire et al. 2007), the seeing, the isoplanatic and isopistonic angles (Elhalkouj et al. 2008).

The principle of the PML instrument is based on the measurement of the angular correlation of wavefront Angle-of-

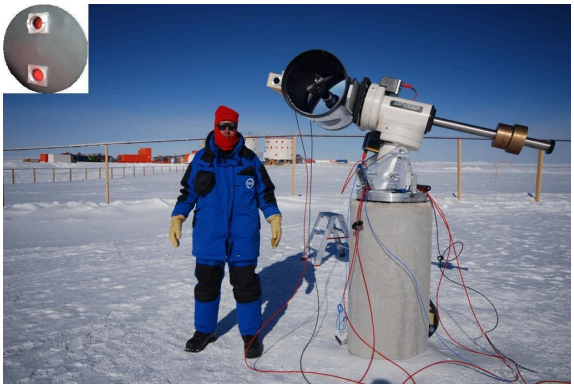

Fig. 1. The PML instrument at Dome C, Antarctica in January 2011. The top-left panel shows the subapertures mask of PML.

Arrival (AA) fluctuations difference deduced from Moon's limb image motion. The AA fluctuations are measured perpendicularly to the lunar limb leading to transverse correlations for different angular separation along the Moon.

The PML instrument consists of a 16-inch telescope (Meade M16) which is installed on an Astrophysics AP3600 mount (Fig. 1). This mount was chosen to avoid overload especially in Dome C conditions. For temperate sites we use an AP1200 mount which is less heavy and cheaper. The pupil mask composed of two sub-apertures of diameter $D = 6cm$ separated by a baseline $B = 26.7cm$, is placed at the entrance pupil of the telescope. The optical device of the PML consists of a collimated beam by using a first lens L1 placed at its focal length from the telescope focus (Figs 2, 3). Two parallel beams are formed at the output of L1 corresponding to each sub-aperture. A Dove prism DP is placed on one of the two beams to reverse one of two images of the lunar edge in order to avoid overlapping bright parts of the Moon (Fig. 4). A second lens L2 is used to form the two images of the Moon limb on a PCO PixelFly CCD camera. Each optical element is placed on a Micro-control plate allowing fine adjustments. To compensate variations in the telescope's focus because of the temperature variations, we installed the CCD camera on an automatic Micro-control plate MP (Fig. 3) controlled by software.

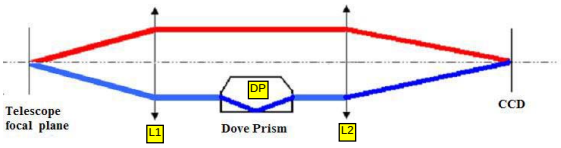

Fig. 2. The optical device of the PML instrument.

Images at the focal plane (Fig. 4) are recorded using a PixelFly CCD camera with 640×480 pixel matrix and $(9.9\times9.9)\mu m^2$ pixel size. The dynamic range of the **analog**/digital conversion is 12 bits. The readout noise is 12 e^- rms and the imaging frequency is 33Hz. In order to freeze atmospheric effects on Moon's limb image motion and to have enough flux, the exposure time was set to 5ms. The spectral response of the camera is maximal for $\lambda = 0.5\mu m$ in a $375 - 550\mu m$ range.

3. Theoretical background

The observation of the lunar limb through two sub-apertures presents two configurations when looking the edge in a direction parallel or perpendicular to the baseline. We use the first configuration to extract the C_N^2 vertical distribution (top-left panel of Fig. 1).

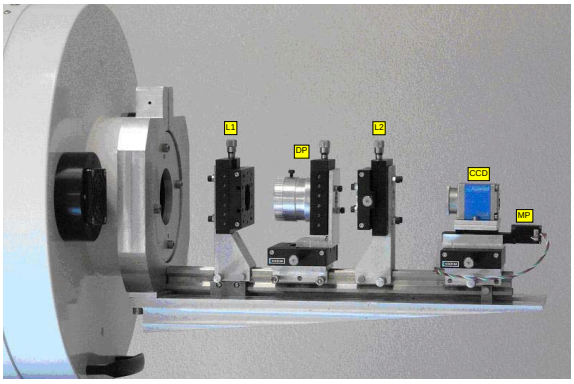

Fig. 3. The focal plane instrument of PML.

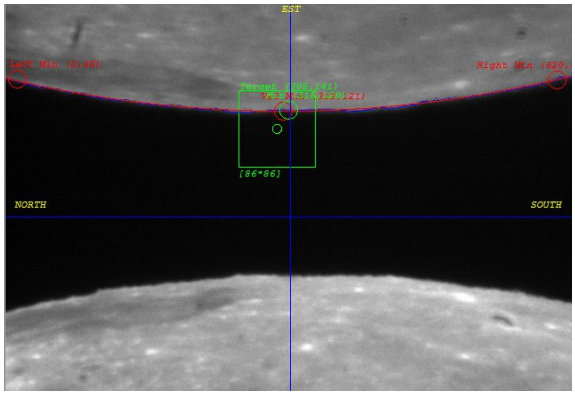

Fig. 4. Example of PML data acquisition.

The transverse covariance of the difference of AA fluctuations α between the two images of the Moon limb (Fig. 4) corresponds to,

$$C_{\Delta\alpha}(\theta) =< [\alpha(r,\theta_0)-\alpha(r+B,\theta_0)][\alpha(r,\theta_0+\theta)-\alpha(r+B,\theta_0+\theta)] > \quad (1)$$

where $B = 26.7cm$ is the baseline between the subapertures, θ is the angular separation along the Moon limb. θ_0 is assumed equal to zero. After development, this expression **is a function** of spatial covariances integrated over the altitude h of the turbulent layers of the whole atmosphere,

$$C_{\Delta\alpha}(\theta) = \int dh C_N^2(h) K_\alpha(B,h,\theta) \quad (2)$$

where

$$K_\alpha(B,h,\theta) = 2\ C_\alpha(\theta h) - C_\alpha(B-\theta h) - C_\alpha(B+\theta h) \quad (3)$$

C_α is the normalized spatial covariance which in the case of the von Kàrmàn model for a baseline ϱ, a sub-aperture diameter D (here 6cm), and a single layer at altitude h is given by Avila et al. 1997 as,

$$C_\alpha(\varrho) = 1.19\ sec(z) \int df f^3 (f^2 + \frac{1}{\mathcal{L}_0(h)^2})^{-11/6} \times [J_0(2\pi f\varrho) + J_2(2\pi f\varrho)][2\frac{J_1(\pi Df)}{\pi Df}]^2 \quad (4)$$

where f is the modulus of the spatial frequency, z is the zenithal distance and $\mathcal{L}_0$ is the outer scale.

Eq.3 represents for a single layer a spatial covariance triplet similar to the SCIDAR one (Fuchs et al. 1998) which is shown in Fig. 5 for a turbulent layer localized at $h = 300m$. The position of the lateral peak ($B = \theta h$) defines the altitude of the layer so that its height leads to the contribution of this layer to the $C_N^2(h)$ profile. For the whole atmosphere we have the superposition of such triplet corresponding to different turbulent layers. The central covariance $C_\alpha(\theta h)$ in Eq.3 could hide the lateral peaks (**dotted** curve in Fig. 5) particularly for high layers (small θ). $C_\alpha(\theta h)$ could be estimated separately from one Moon limb. One can have two estimates of this central covariance from each Moon limb and use the mean one. The substraction of $2 * C_\alpha(\theta h)$ from the triplet in Eq.3 leads directly to lateral peaks $[-C_\alpha(B-\theta h) - C_\alpha(B+\theta h)]$. For the whole atmosphere we have the superposition of such lateral peaks with different positions and weightings corresponding to the different turbulent layers in the atmosphere.

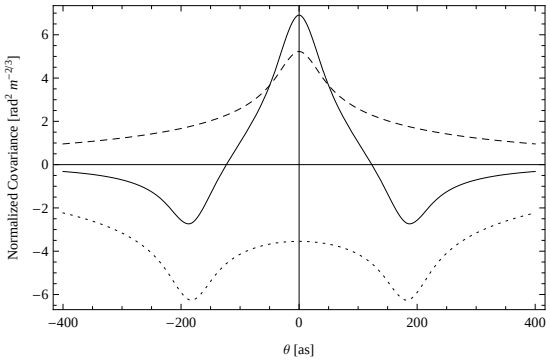

Fig. 5. Triplet of spatial covariances for a single turbulent layer localized at an altitude $h = 300m$ (solid line). The curve in dashed line indicates the central spatial covariance $C_\alpha(\theta h)$ in Eq. 3. In dotted line, we have the difference $[K_\alpha(B,h,\theta) - 2\ C_\alpha(\theta h)]$ leading to lateral peaks $[-C_\alpha(B-\theta h) - C_\alpha(B+\theta h)]$.

Thus, the extraction of the $C_N^2(h)$ profile from the PML is obtained from the estimation of the whole atmosphere lateral peaks obtained by this difference:

$$Y(\theta) = C_{\Delta\alpha}(\theta) \ - \ 2 \times \int dh C_N^2(h) C_\alpha(\theta h) \tag{5}$$

In a matrix form, one can write,

$$Y = M \times c \tag{6}$$

where c is vector of the sampled $C_N^2(h_i)$ profile and M is a matrix obtained from the difference $[K_\alpha(B,h_i,\theta_j) - 2\ C_\alpha(\theta_j h_i)]$ for different altitude h_i and angular separations θ_j.

4. Data processing & results

The first step of PML data processing is to retrieve accurately AA fluctuations from Moon's limb motion (transverse AA fluctuations). After processing on each image a flat and dark field correction, each image $I(x,y)$ is slightly blurred with a median filter on 3×3 pixel blocks. It avoids possible outliers due to Poisson noise or Moon's small features with relative high intensity differences that can affect the detection of the limb. This type of filtering is more effective than convolution when the goal is to simultaneously reduce noise and preserve edges (Pratt 1978).

Then, the image with the two Moon's limbs is separated on two images with top and bottom edges (Fig. 4). On each half-image, a spatial gradient $G(x,y)$ is processed by convolution with a 3×3 Prewitt edge detector (Pratt 1978) defined as $P = \begin{pmatrix} -1 & -1 & -1 \\ 0 & 0 & 0 \\ 1 & 1 & 1 \end{pmatrix}$, or $-P$ if y-axis points to the Moon center. Detection of the limb position in absolute value of the image gradient is determined by a centroid calculation over each column.

We process $N = 1000$ images (acquisition of $1min$) that gives two sets of Moon limb angular positions corresponding to top and bottom of lunar edge in Fig. 4. Then, a transverse covariance of the difference of the AA fluctuations $C_{\Delta\alpha}(\theta)$ between these two Moon limbs as given in Eq. 1 is deduced. This differential variance calculated for each image has the practical advantage of being insensitive to vibration effects of the telescope, wind shaking and tracking errors. In the other hand, from top and bottom limbs, we deduce separately two estimations of the central covariance $C_\alpha(\theta h)$ integrated over the whole atmosphere. Twice of the mean of these central covariances is then subtracted from $C_{\Delta\alpha}(\theta)$ as indicated in Eq. 5 leading to lateral covariance estimator Y (Fig. 6). This latter and all these covariances are obtained for each pixel along $\sim$ 620 pixels of the CCD camera ($\sim$ 20 pixels are lost when recentring Moon limbs on CCD due to the mount drift). Each pixel corresponds to $\simeq 0.57''$ leading to a total field of more than $350''$.

Retrieving $C_N^2(h)$ profile from the transverse covariance estimator Y is an inverse problem as indicated in Eq. 6. The estimated $C_N^2(h)$ is obtained by minimization of the **least** squares criterion $J = \|Y - Mc\|^2$ under positivity constraint using an iterative gradient method (Bertero & Boccacci 1998). A diagonal weighting matrix with Y variances is used in order to favour the steadier measurements.

The PML instrument has been installed first at the Dome C site in Antarctica for a long campaign measurement for the whole year 2011. But due to a very limited internet connection of Concordia station, we didn't have access to the PML database. We had to wait the summer campaign to recover it (May 2012). Since this time, the data processing of this campaign is continuously in progress and an example of the first profiles obtained on two data sets are shown in Fig. 7 compared to median profile of radio-sounding balloons obtained during the 2005 winter campaign (Trinquet et al. 2008). **The variation of the balloon data are represented by the** 10% **and** 90% **percentiles of the measured profiles during this 2005 campaign (dotted lines in Fig. 7). A direct comparison of these results is meaningless but these first results show that the instantaneous measurements of PML are consistent with the general behaviour of the Dome C atmosphere as indicated by radio-sounding balloon's profiles**. Indeed, the Fried's parameter deduced from the PML profile in Fig. 7 is $r_0 = 8.2cm$ for 16h45UT profile and $r_0 = 7.5cm$ for 17h17UT **while the median profile of balloons from 2005 campaign** leads to $r_0 = 6.7cm$. Figure 6 shows the measured lateral covariance $Y(\theta)$ (solid line) as indicated in Eq. 5. One can note that for large θ, the measured covariance $Y(\theta)$ is more fluctuating due to less sampling.

The $C_N^2(h)$ profiles in Fig. 7 are deduced by comparison of the measured lateral covariance $Y(\theta)$ and the modeled one (Fig. 6). These profiles (Fig. 7) are obtained with a variable vertical resolution. Indeed, the altitude is inversely proportional to angular separation θ with a maximum of more than $350''$. Then, the resolution is higher in the ground layer than in the free atmosphere. The resolution used for the first Dome C results (Fig. 7)

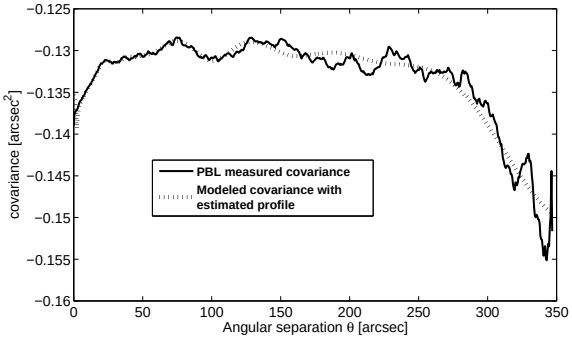

Fig. 6. Example of lateral covariance $Y(\theta)$ obtained with PML at Dome C in Antarctica on January 25th, 2011 at 16h45 UT (solid line). The PML extracted $C_N^2(h)$ profile is obtained by modeling angular covariance (dotted line) leading to the best fit of the measured one (solid line).

is: $\Delta h = 100m$ for the ground layer ($h \leq 1km$); $\Delta h = 500m$ for the low free atmosphere ($1km < h < 5km$); $\Delta h = 1000m$ for the mid-free atmosphere ($5km < h < 15km$) and $\Delta h = 2000m$ for the high free atmosphere ($h > 15km$). The highest altitude h_{max} measured with the PML is more than $50km$. But, we limited h_{max} to $25km$ for comparison with balloons profiles reaching only $20km$ (Fig. 7). On the other hand, due to a limited field-of-view the PML instrument has a minimum altitude detectable. Indeed, the maximum of the lateral peak (Fig. 5) detectable is around $150m$ for the field-of-view of PML which is more than $350''$ ($B = \theta h$). As shown in Fig. 5, even if the maximum of lateral peak is not in the field-of-view, the corresponding layer is detectable if we take into account the **expansion** of the covariance curves. Then, if we consider an outer scale of $10 - 100m$ (baseline at which the spatial covariance in Eq. 4 tends to zero), the minimum altitude is fixed to $100m$. The contribution of the lowest layer $0 - 100m$ is obtained by the difference between the profile deduced from the inversion of the PML covariances (Fig. 6) and the total seeing from DIMM method (Sarazin & Roddier 1990) using PML data. For the total seeing obtained from PML, we have about 620 estimations (each point the Moon limb lead to a DIMM measurement) and we keep only the median one.

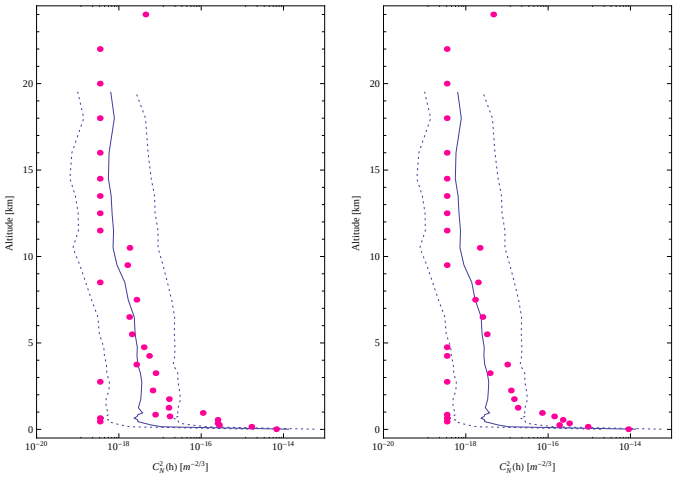

Fig. 7. Example of C_N^2 profile (dots) from PML at Dome C in Antarctica on January 25th, 2011 at 16h45UT (left panel) and 17h17 (right panel). For comparison, the median profile (solid line) of radio-sounding balloons obtained during the 2005 winter campaign is plotted in solid line. **Dotted lines indicate the** 10% **and** 90% **percentiles of balloon's data.**

The error sources of PML monitor are similar to those affecting the MOSP instrument which are hugely described in Sect. 3.3 of Maire et al. 2007. These errors are mainly related to the detection of the Moon limb position due to photon noise. For the evaluation of the error of this photon noise we used the same simulation described in Maire et al. 2007. The Moon limb images are simulated by a 2D Heaviside function. The Fourier Transform (FT) of this latter is multiplied by the atmospheric short-exposure transfer function to introduce the seeing conditions and by the aperture transfer function. The 2D inverse FT of this product leads to simulated images of Moon's limb for given seeing conditions and PML aperture filtering. Then, the photon noise is added as Poisson distribution using the mean value of intensity of each pixel as obtained with the PML observations. These Moon's limb images pass through the PML data processing described in Sect. 4. The lateral covariance in Eq.5 of Moon's limb fluctuations due to photon noise is calculated for each realization and the mean one is deduced from $N = 1000$ **samples. As Moon's limb fluctuations due to photon error are considered uncorrelated from the atmospheric ones, this lateral covariance is added to the theoretical one using Eqs.2,4 and 5 and the median radio-sounding balloon profile (Fig.7). The error on the lateral covariance due to the photon noise is at maximum** 0.5% **in the seeing conditions of the results presented in Fig.7. The noisy lateral covariance is then inverted to retrieve the** $C_N^2(h)$ **profile as in the PML instrument. Comparisons with the injected profile which is no more than the median profile** $C_{N,Bal}^2(h)$ **of radio-sounding balloons is evaluated using a relative error defined as** $E_{ph} = \sum_{i=1}^{n} \mid C_{N,Bal}^2(h_i) - C_N^2(h_i) \mid / \sum_{i=1}^{n} C_N^2(h_i)$ **over** n **retrieved layers.** Eph **is about** $\sim 4\%$ **representing a typical low error for such instrument.**

5. Conclusions

The advantage of the PML instrument is that in addition to the $C_N^2(h)$ profile extracted with high vertical resolution using an easy and undemanding technique, it is able to provide other parameters of turbulence **particularly the profile of the outer scale using the same technique described in Maire et al. 2007. Estimations of the isoplanatic and isopistonic domains (Elhalkouj et al. 2008) from the PML instrument are also possible**. On the other hand, the PML is also applicable to solar limb by use of a density filter. The first PML results obtained with solar limb at Dome C are also available which will be presented in a next separate paper.

Acknowledgements. We would like to thank the Polar Institutes IPEV and PNRA, the National Institute for Earth Sciences and Astronomy INSU and the French Programme of High Angular Resolution ASHRA for logistical and financial support for the development and the installation of the PML instrument at the site of Dome C in Antarctica. We wish also to thank warmly Alex Robini for his precious help and we are very grateful for his dedication to the success of the PML. We thank the technical team of the winterover 2011 for its help.

References

Ellerbroek, B. 2011, 2nd International Conference AO4ELT, Victoria
Hubin, N. 2011, 2nd International Conference AO4ELT, Victoria
Costille, A. & Fusco, T. 2011, 2nd Conference AO4ELT, Victoria
Azouit, M. & Vernin, J. 2005, PASP, 117, 536
Fuchs, A. , Tallon, M. & Vernin, J. 1998, PASP, 110, 86
Sarazin, M. & Roddier, F. 1990, A&A, 227, 294
Avila, R., Ziad, A. , Borgnino, J., et al. 1997, JOSA A, 14, 3070
Pratt, W. K. 1978, A. Wiley-Interscience Publication, New York

Bertero, M. & Boccacci, P. 1998, IOP Publishing, Bristol
Trinquet, H., Agabi, A., Vernin, J., et al. 2008, PASP, 120, 203
Maire, J., Ziad, A., Borgnino, J., et al. 2007, MNRAS, 377, 236
Elhalkouj, T., Ziad, A., Petrov, R. G., et al. 2008, A&A, 477, 337